Carbohydrate Polymers 86 (2011) 505–512

Contents lists available at ScienceDirect

Carbohydrate Polymers

journal homepage: www.elsevier.com/locate/carbpol

Paclitaxel loaded electrospun porous nanofibers as mat potential application for chemotherapy against prostate cancer

Guiping Ma[a,*], Yang Liu[a,b], Cheng Peng[a,b], Dawei Fang[a,b], Baojiang He[c], Jun Nie[a]

[a] State Key Laboratory of Chemical Resource Engineering, Key Laboratory of Carbon Fiber and Functional Polymers, Ministry of Education, Beijing University of Chemical Technology, Beijing, 100029, PR China
[b] School of Materials Science and Engingeering, Changhzou University, Changzhou, Jiangsu, 213164, PR China
[c] Zhengzhou Tobacco Institute of CNTC, Zhengzhou, 450001, PR China

ARTICLE INFO

Article history:
Received 11 March 2011
Received in revised form 18 April 2011
Accepted 27 April 2011
Available online 27 May 2011

Keywords:
Chitosan
Electrospinning
Paclitaxel
Porous nanofibers
Hyaluronic acid

ABSTRACT

A highly porous chitosan nanofibers were obtained by electrospinning chitosan/polyethylene oxide (PEO) blend solutions and then removing PEO with water. The porous morphology of the nanofibers was observed by scanning electron microscopy. The porous nanofibers were soaked in 0.1 wt% paclitaxel solution to load the cancer drug. Then a polyanion nature macromolecular hyaluronic acid (HA) was encapsulated on the chitosan polycation porous nanofibers by immersing the fibers into a 4 wt% HA aqueous solution. Differential scanning calorimetry (DSC) and Fourier transform infrared (FT-IR) were used to investigate the polymer formation and the interaction among two nature macromolecular and the cancer drugs. The paclitaxel release profiles of the encapsulated fibers in PBS were analyzed by UV–vis spectrophotometer. In vitro DU145 prostate cancer cells activities of the nanofibers were examined by MTT. Cell culture results showed that the PTX-loaded nanofibers mats were good in prohibiting the cell attachment and proliferation. These results strongly suggested that the chitosan/hyaluronic acid fibers had an effect of controlled release of paclitaxel and were suitable for postoperative chemotherapy of prostate cancers.

1. Introduction

Electrospinning is a well recognized and effective technique to produce fibers with diameters in the range of micrometers down to tens of nanometers from the electrostatically driven jets of polymer solution or melts (Bhattarai et al., 1996; Reneker & Chun, 1996; Li, Wang, & Xia, 2004). The unique properties of electrospun nanofibers such as high special surface area, high area to volume ratio and small porous, have enabled nanofibers many applications that include filtration (Woon, Fong, Hung, & Yuen, 2010), nanofiber reinforcement (Huang, Zhang, Ramakrishna, & Lim, 2004), wound healing (Kurpinski, Stephenson, Janairo, Lee, & Li, 2010), tissue engineering (Hong & Madihally, 2010; Yoo, Lee, Yoon, & Park, 2005), and release of drugs (Im, Yun, Lim, Kim, & Lee, 2010). In recent decades, a wide range of natural product materials, like hyaluronic acid, collagen, gelatin and chitosan, and a wide variety of synthetic biodegradable polymers, such as poly(L-lactide) (PLLA), polyethylene oxide (PEO) and polycaprolactone (PCL), and co-polymers, such as poly(L-lactide-co-caprolactone) and poly(lactic-co-glycolic acid) (PLGA), have been electrospun in order to meet different requirements for specific applications in tissue engineering and drug delivery (Bhattarai, Edmondson, Veiseh, Matsen, & Zhang, 2005; Shalumon et al., 2009; Sill & Recum, 2008; Sujata, Chung, Khetan, & Burdick, 2008; Yang, Murugan, Wang, & Ramakrishna, 2005). In particular, the nanofibers are very favorable for the adsorption of liquids and for preventing bacteria penetration and thus provide good conditions for post-surgical chemotherapy (Zhou et al., 2008).

Hyaluronic acid (HA) is a naturally occurring straight anionic polysaccharide and a linear polysaccharide of alternating D-glucuronic acid and N-acetyl-D-glucosamine, which widely exists in many connective tissues (e.g., cartilage) (Allison & Grande-Allen, 2006; Meyer, 1947). HA plays a role in cellular processes like cell proliferation, morphogenesis, inflammation, wound repair and interacts with cells through surface receptors (Chen & Abatangelo, 1999; Toole, 2004). These biological interactions make HA a candidate for the development of biomaterials that can directly interact with cells. HA has attracted much attention for its remarkable applications in tissue engineering, wound healing and release of drugs due to its biodegradability, biocompatibility and wound healing ability.

Chitosan is a natural, cationic amino polysaccharide copolymer of glucosamine and N-acetylglucosamine, obtained by the alkaline, partial N-deacetylation of chitin which is commercially extracted

* Corresponding author. Tel.: +86 1064421310; fax: +86 1064421310.
E-mail address: magp0539@163.com (G. Ma).

0144-8617/$ – see front matter © 2011 Elsevier Ltd. All rights reserved.
doi:10.1016/j.carbpol.2011.04.082

from exoskeleton of crustacean, e.g., crab, shrimp, etc. It is the most important natural polysaccharide after cellulose (Fernando & Sérgio, 2004; Yui, Kobayashi, Kitamura, & Imada, 1994). Chitosan has several biological properties that make it an attractive material for use in medical applications such as biodegradability, lack of toxicity, antifungal effects, wound healing acceleration, biocompatibility, and immune system stimulation (Blasinska & Drobnik, 2008; Khor & Lim, 2003; Senel & McClure, 2004). Electrospinning of chitosan-based formulations containing good fiber-forming polymers like PEO, polyvinylalcohol (PVA), or polyvinylpyrrolidone (PVP) (with quaternized chitosan) have been widely documented.

Drug delivery systems have been developed by using polymeric materials in the form of microparticle, hydrogel and micelle (Manna, Bharani, & Patil, 2009; Worrall, Sudarisman, & Priadi, 2009). Recently, drug-loaded electrospun fibers with higher drug encapsulation efficiency and better stability than other drug formulations have attracted a great deal of attention (Tiwaria, Tzezanab, Zussmanb, & Venkatramana, 2010). The electrospun nanofibers possess high surface-to-volume ratio which would accelerate the solubility of drug in the aqueous solution and enhance the efficiency of the drug.

Paclitaxel (PTX) is a well known mitotic inhibitor and radiosensitizing agent (Ranganath & Wang, 2008) used in cancer chemotherapy but with poor water solubility. Its mechanism of action comprises of interaction with microtubule degradation resulting in increased mitotic arrest, decrease in cellular motility, and disruption in intercellular signal transmission.

Here we presented the development and characterization of a natural–natural polymeric nanofiber as a drug carrier with the combined advantages, comprised of well-blended chitosan and hyaluronic acid. The first advantage of this study lay in the in situ formation of porous electrospun nanofibers and PTX nanoparticles encapsulated in the pores. The second advantage was the interaction between the positively charged porous polymer (CS) nanofibers and negatively charged polymers (HA), which had no side effects or adverse reactions resulted from crosslinking with glutaraldehyde or by photopolymerization (Chen, Wang, Wei, Mo, & Cui, 2010; Theron et al., 2010; Zhang, Venugopal, Huang, Lim, & Ramakrishna, 2006). The morphology of pores, and drug loaded nanofiber, and the actual PTX release characteristics were investigated systematically. The structure and interaction of the fibers were subjected to detailed analysis by differential scanning calorimetry (DSC) and Fourier transform infrared (FT-IR). The potential use of this as-spun fiber mat as a scaffolding material for postoperative chemotherapy of prostate cancers was evaluated in vitro against DU145 prostate cancer cells. Cell culture results showed that nanofibers mats were good in prohibiting the cell attachment and proliferation.

2. Experimental

2.1. Materials

HA used in this study was purchased from Dali Hyaluronic acid Co., Ltd of Liuzhou Chemical Group (Liuzhou, Guangxi, China) with the molecular weight of 1 000 000 g mol^{-1}. Chitosan (CS) with molecular weight of 1 00 000 g mol^{-1} from crab shell was purchased from Yuhuan Ocean Biochemical Co., Ltd (Zhejiang, China) and used as received. PEO with molecular weight of 900 000 g mol^{-1} was supplied by Acors Organics (Shanghai, China). Paclitaxel of 99.9% purity was purchased from Xi'an Bio-sep Biotechnology (Xi'an, China). Acetic acid was supplied by Zhejiang Sunrise Chemicals Co., Ltd (Zhejiang, China) with HPLC grade. All other materials and reagents used were of analytical grade.

2.2. Fabrication of nanofibers

A 5.0% (w/w) PEO solution was prepared by dissolution of 5.0 g PEO in 100 mL distilled water at room temperature with vigorous stirring. CS (5.0 g) was dissolved in 100.0 g of 2.0% (w/w) acetic acid solution. The PEO and chitosan were blended with different weight ratios, but the total polymer concentration was kept at 5.0% (w/v) in all experiments.

The mixed solution was pumped at a predetermined rate using a syringe pump (WSZ-50FZ, Zhejiang University Medical Instrument Co., Ltd) at a constant rate of 0.3 mL h^{-1}, forming a bead of solution at the tip of syringe. A high voltage difference (12–20 kV) was applied between the nozzle needle with diameter of 0.57 mm, a negative potential, and a grounded collection target. As the jet breaks up into fibers from the Taylor Cone, the liquid was evaporated and gave rise to relatively dry fibers which were subsequently spun on the aluminum foil wrapped rotating shaft until multilayered fiber mat was obtained.

The blend fibers were soaked in distilled water for 10 h in order to remove PEO and got the porous nanofibers. Then porous nanofibers were soaked in the ethanol solution of paclitaxel (0.1 wt%) for 8 h in order to make the drugs adhesive in the fiber. At last the fibers were soaked in the HA solution (4 wt%) to let the CS and HA attacked relying on the attraction between positive and negative charges.

2.3. Nanofibers characterization

2.3.1. Morphology analysis

The morphology of the medicated electrospun fibers was observed by using Hitachi S-4700 scanning electron microscope (Hitachi Company, Japan), and its accelerating voltage was 20 kV. Samples were mounted on metal stubs using a double-sided adhesive tape and vacuum-coated with a gold sputtering layer prior to examination. Diameters and distributions of the electrospun fibers were analyzed from the SEM images by using Image J analysis software (Image J, National Institutes of Health, USA).

2.3.2. FT-IR analysis

FT-IR spectrum was recorded on Nicolet 5700 instrument (Nicolet Instrument, Thermo Company, USA). Samples were prepared as nanofiber membranes and were scanned against air background at wavenumbers range 4000–500 cm^{-1} with resolution of 4.0 cm^{-1}. The peaks area was calculated by a software ominc 32.

2.3.3. Differential scanning calorimetry (DSC)

The thermal analysis of the electrospinning fibers was studied by a DSC 204 F1 thermal analysis system (Netzsch, Germany). Samples sealed in aluminum pans were heated from room temperature to 270 °C at a heating rate of 10 °C/min under 30 mL/min of nitrogen flow.

2.3.4. Fluorescence microscope

The image of the electrospun fibers suspension after PTX loading was taken by an inverted fluorescence microscope (Olympus IX81) excited 270 nm in UV light. The samples were positioned so that the emitted light was detected at 270 nm from the incident beam.

2.4. In vitro paclitaxel release

In vitro paclitaxel release test was conducted by immersing fiber discs/sheets weighing 3 mg each into 5 mL PBS buffer (pH 7.4) in 15 mL centrifuge tubes and incubated at 37 °C and 100 rpm in a shaking water bath (GLS Aqua 12, Shanghai, China) to simulate body physiological conditions. At each fixed time interval, 2.0 mL released solution was withdrawn from the dissolution medium

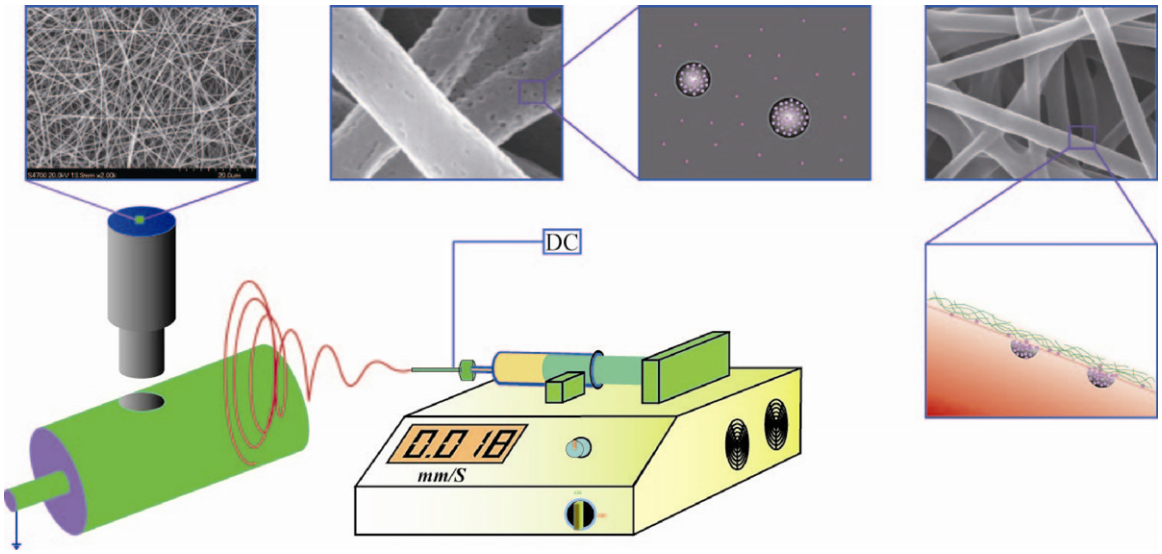

Fig. 1. Sample preparation process for porous, PTX loaded, and HA encapsuled blend fibers by electrospinning.

after incubation, while an equal amount of fresh PBS was added back to the incubation solution. The amount of paclitaxel was detected by a Hitachi U-3010 UV-vis spectrophotometer (Hitachi High Technologies Corporation, Tokyo, Japan), a maximal absorption peak of 270 nm was observed for freshly prepared paclitaxel in PBS and released within the designed period. For standard samples with a concentration from 0 to 30 μg/mL, a linear correlation ($\gamma^2 = 0.9999$) was determined between the absorption strength and paclitaxel concentration. The percentage of the released drug in samples was then calculated based on the initial weight of the drug incorporated in the electrospun nanofibers (Ranganath & Wang, 2008).

2.5. In vitro cytotoxicity of drug-loaded fiber mats

2.5.1. Methylthiazolydiphenyl-tetrazolium bromide (MTT) assay

The cytotoxicity of the electrospun fiber membranes was evaluated based on a procedure adapted from the ISO10993-5 standard test method. DU145 prostate cancer cells were cultured in RPMI1640 medium supplemented with 10% fetal bovine serum, together with 1.0% penicillin–streptomycin and 1.2% glutamine. Culture was maintained at 37 °C in a wet atmosphere containing 5% CO_2. When the cells reached 80% confluence, they were trypsinized with 0.25% trypsin containing 1 mM ethylenediamine tetraacetic acid (EDTA). The viabilities of cells were determined by the MTT (3-[4,-dimethylthiazol-2-yl]-2,5-diphenyltetrazolium bromide; thiazolyl blue) assay. The level of the reduction of MTT into formazan can reflect the level of cell metabolism. For the MTT assay, the as-spun membranes were sterilized with highly compressed steam for 15 min and placed in wells of a 24-well culture plate, respectively. The samples were then incubated in 1 mL of RPMI1640 medium at 37 °C for 24 h. The extraction ratio was 6 cm^2/mL. At the end of this period, the membranes were removed and the so-called extracts were obtained and further were diluted to obtain extraction medium samples. DU145 prostate cancer cells were seeded in wells of a 96-well plate at a density of 4×10^3 cells per well. After incubation for another 24 h, the culture medium was removed and replaced with the as-prepared extraction medium and incubated for 24 h, then 150 μL of MTT solution was added to each well. After 24 h incubation at 37 °C, 200 μL of dimethyl sulfoxide was added to dissolve the formazan crystals. The dissolved solution was swelled homogeneously for about 10 min by the shaker. The optical density of the formazan solution was detected by an ELISA reader (Multiscan MK3, Labsystem Co. Finland) at 570 nm. For reference purposes, cells were seeded to medium a fresh culture medium (negative control) under the same seeding conditions, respectively.

2.5.2. Cell culture and adhesion

DU145 prostate cancer cells were selected for the biological assays in order to evaluate the effect of electrospun fiber membranes on cell culture, adhesion, and proliferation. The electrospun fiber membranes were fixed on the glass cover slips by using copper tapes. The sample membranes were sterilized, rinsed three times with sterile phosphate buffer solution (PBS), then transferred to individual 24-well tissue culture plates. Aliquots (1 mL) of DU145 prostate cancer cells suspension with 1.5×10^4 cells/mL were seeded on the sample membranes. After 24 h of culture, cellular constructs were harvested, rinsed twice with PBS to remove non-adherent cells. The samples were dehydrated through a series of graded ethanol solutions and dried overnight at room temperature. The dry samples were coated with gold by sputtering for further analysis cell morphology on the surface of the scaffolds by SEM.

3. Results and discussion

3.1. SEM images

The preparation process for porous, loaded PTX, and encapsulated blend nanofibers with HA by electrospinning were shown in Fig. 1. Fig. 2 illustrated SEM micrographs of electrospun nanofibers. The original electrospinning product showed non-woven nanofibers structure. The electrospun CS/PEO blend nanofibers with average fiber diameter of 300 nm and narrow diameter distribution showed the round-shaped and smooth morphology in Fig. 2(d). Previous research reported that electrospun blend nanofibers and prepared porous nanofibers via selective dissolution of one component (Bognitzki, Frese, Steinhart, Greiner, & Wendorff, 2001; You et al., 2006). In this study, similarly, PEO was removed from the ultrafine CS/PEO blend nanofibers via a selective dissolution technique. After dissolution, the large amount of porous with circular shape and narrow size distribution formed on the surface of nanofibers. The nanofibers mat was immersed into HA aqueous solution (1 mg/mL) for 10 h. The morphology of encapsulated HA nanofibers were shown in Fig. 2(c), the nanofibers

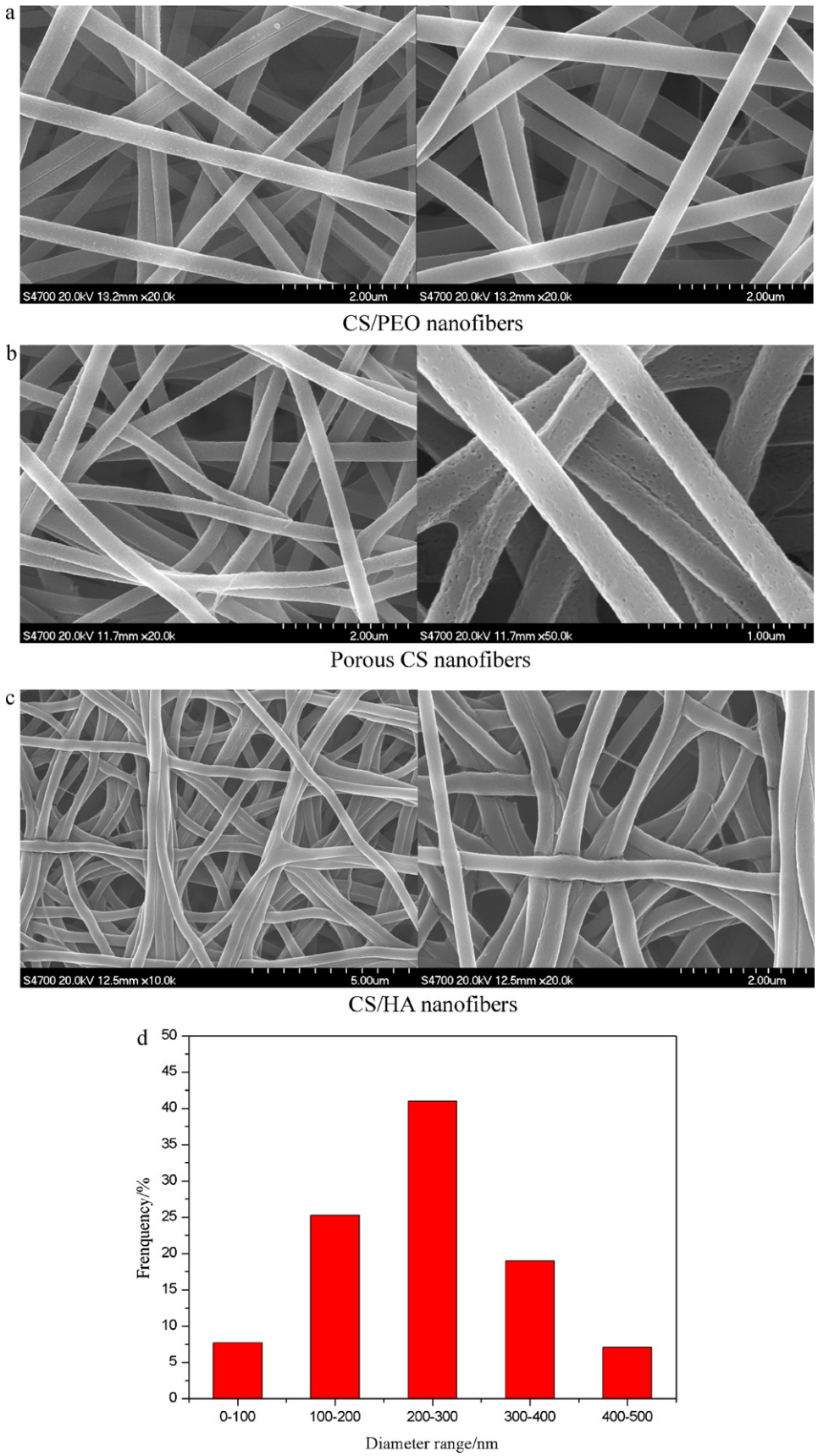

Fig. 2. SEM images of electropsun composite nanofibers: (a) CS/PEOnanofibers; (b) CS porous nanofibers; (c) PTX-loaded CS/HA nanofibers; (d) Diameter distributions of CS/PEO nanofibers.

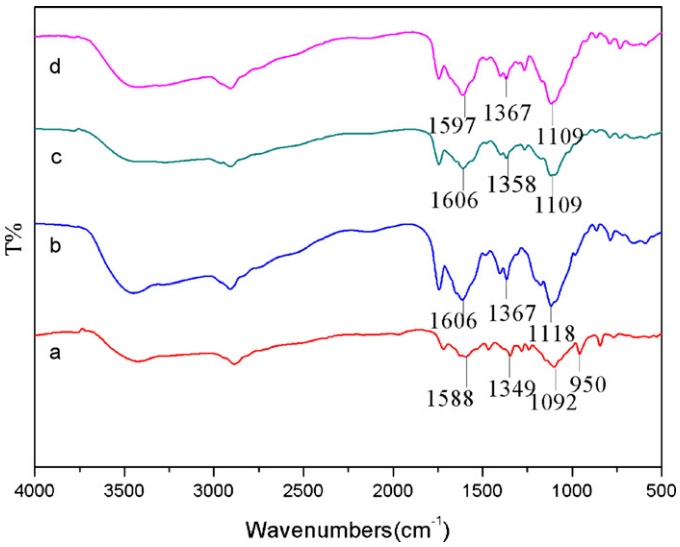

Fig. 3. FT-IR spectra of electrospun nanofibers: (a) CS/PEO nanofibers; (b) porous CS nanofibers; (c) PTX-loaded porous CS nanofibers; and (d) PTX-loaded CS/HA nanofibers.

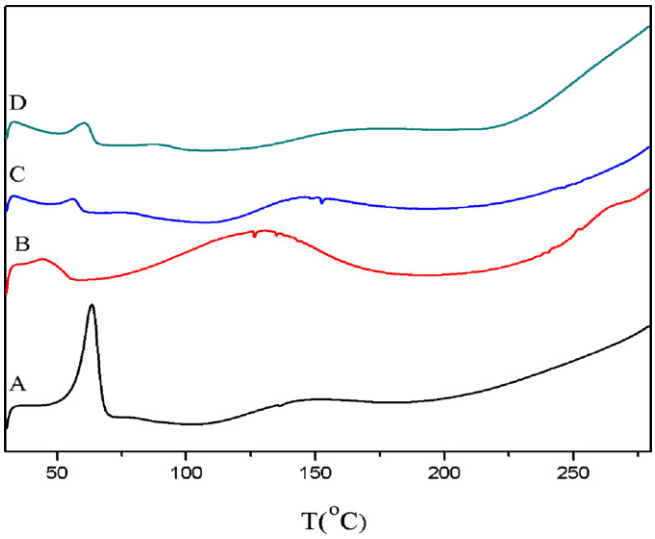

Fig. 4. DSC thermograms curves of electrospun nanofibers: (a) CS/PEO nanofibers; (b) porous CS nanofibers; (c) PTX-loaded porous CS nanofibers; and (d) PTX-loaded CS/HA nanofibers.

morphology of the nanofibers was maintained and the nanofibers were orderly distributed as before encapsulation which meant that HA films were formed on the surface of the nanofibers. The negatively charged nature polymer (HA) was assembled on the positively charged nature polymer (CS) nanofibers surface. PTX was encapsulated between them, and the interaction increased nanofibers strength (Pan, Ge, & Gu, 2007).

3.2. FT-IR spectroscopy

FT-IR spectra of the nanofibers were shown in Fig. 3. The broad peak at 3430 cm^{-1} was due to N–H and hydrogen bonded O–H stretching on the CS back bone. The N–H deformation vibration absorption peak was observed at 1606 cm^{-1} and –C–O–C peak appeared at 1109 cm^{-1}, respectively (Velde & Kiekens, 2004). The in-plane bending vibration (1367 cm^{-1}) of –OH on the backbone of CS was used as interior label to investigate the changes of peaks' intensity. The peaks at 1106 cm^{-1} and 950 cm^{-1} were due to stretching of the C–O–C group in PEO (Wongsasulak, Kit, McClements, Yoovidhya, & Weiss, 2007). In Fig. 3(a) and (b), comparing these two spectra, one could find after selective wash treatment by water, the area ratio of A_{1106}/A_{1367} was decreased from 5.419 (Fig. 3(a)) to 4.574 (Fig. 3(b)), it means that most of the PEO was removed. The spectra of PTX-loaded porous nanofibers (Fig. 3(c)) were similar with the spectra in Fig. 3(b). It may be caused by the little amount of the PTX loaded on the fibers that could not be detected by FT-IR. After encapsulation with HA, the absorption peaks of –N–H shift from 1606 to 1597 (Fig. 3(d)). It proved that the special interaction of CS and HA via electrostatic was formed.

3.3. DSC results

Fig. 4 presented DSC data for electrospun nanofibers of CS/PEO, before and after PEO removal. The first characteristic endothermic peaks at 64 °C of CS/PEO could be dehydrated or denaturalized when they were heated. The endothermic curve of CS/PEO blend nanofibers was broad, and the peak shifted toward lower temperatures comparing with the pure chitosan and PEO. It indicated that the aggregation structure of CS/PEO was amorphous, and chains were in the noncrystalline state due to the rapid solidification process during electrospinning. However, the endothermic peaks were shifted to higher temperature and the peak becomes sharp after the porous CS nanofibers were loaded on the PTX, and encapsuled by HA, which was caused by the interaction of positive and negative charges between CS and HA. This amorphous nature of the PTX might have pronounced pharmaceutical significance as it could lead to increased solubility and improve the biological activity (Mu, Teo, Ning, Tan, & Feng, 2005).

3.4. Fluorescence image

Fig. 5 presented the fluorescence image for the PTX-loaded CS/HA nanofibers. The results demonstrated the fluorescence of the nanofibers, indicating the presence of PTX. The dark regions in the image, as in all of the fluorescence images, were areas that were out of focus due to the uneven contour of the electrospun sample. The fluorescence images results suggested that the PTX was presented not only in the inside of fiber porous but also in the encapsulated sections of the nanofibers matrix. But, all fluorescence microscopy images indicated that PTX was presented throughout the depths of the electrospun matrix, suggesting a fairly uniform dispersion of PTX owing to the uneven porous size and distribution. These results suggested a slight improvement in PTX incorporation in the CS/HA nanofibers and the nanofibers porous permitted the incorporation of slightly more PTX encapsulated in the nanofibers than the smooth fibers.

3.5. Drug release

In vitro release profiles of paclitaxel from the PTX loaded nanofibers was shown in Fig. 6. The release rate of PTX in phosphate buffered saline (PBS) solutions was examined by immersing PTX loaded electrospun fiber mats into solutions with pH of 7.4. A burst release was observed from the release profile due to the diffusion-controlled release of the drug and the higher water adsorption of the electrospun nanofibers, moreover, the nanofibers possessed the high surface area, porous, allowing more drug molecules to diffuse from the nanofibers to the surrounding medium (Meng et al., on line), therefore the drug molecule had a more rapid diffusion from the matrix into the aqueous medium. After 48 h, it took short time to reach the equilibrium, the release curves of PTX deviated from the curve, and the rates became slower. This may be due to the role of positive and negative charges to prevent the PTX drug to release from the nanofibers. The cure was near constant release

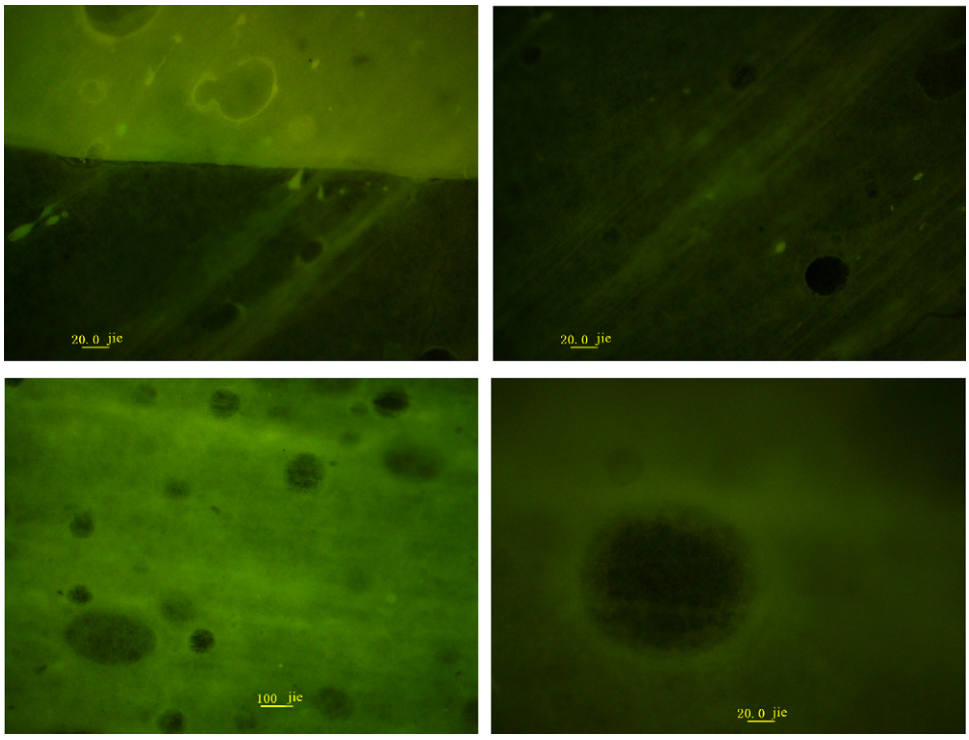

Fig. 5. Fluorescence image of PTX-loaded CS/HA nanofibers.

rate and longer drug release sustainability which might be crucial for treating prostate cancer.

3.6. MTT assay

A biomaterial should not release toxic products and support cellular attachment, which could be evaluated through in vitro cytotoxic tests. The level of toxicity of these nanofibers scaffolds towards cell viability was evaluated using ISO10993-5 standard test method of indirect MTT assay. The absorbance of the samples was read at 570 nm in a spectrophotometer (Fig. 7). The extraction media were prepared from the nanofibers scaffold washed with PBS three times. When cells were incubated with extracts obtained from washed scaffold, the viability of cells was changed with the change of PTX concentration. The viability of the DU145 prostate cancer cells after 48 h of incubation with the PTX-loaded CS/HA electrospun nanofibers was significantly lower than that of nanofibers that were loaded lower paclitaxel concentration for the same culture period. The higher concentration of extraction media was, the stronger inhibition affected on cells. When cells were incubated with 100% extract obtained from washed nanofibers, there was a significant decrease on cell viability compared to 50, 25, and 10%. The obtained results suggested that electrospun nanofibers of CS/HA were nontoxic to DU145 prostate cancer cells and are good candidates to be used as wound dressing for post-surgical chemotherapy.

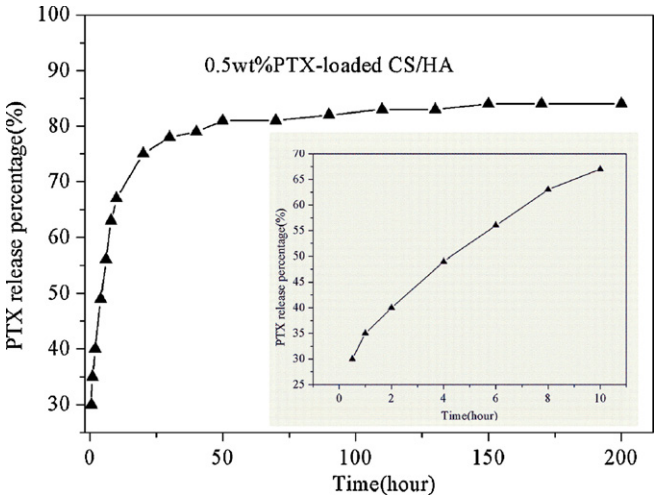

Fig. 6. In vitro release profiles of paclitaxel from the encapsulated nanofibers by immersing the fibers (0.5 wt% PTX loaded) into PBS buffer solution (pH 7.4) at 37 °C.

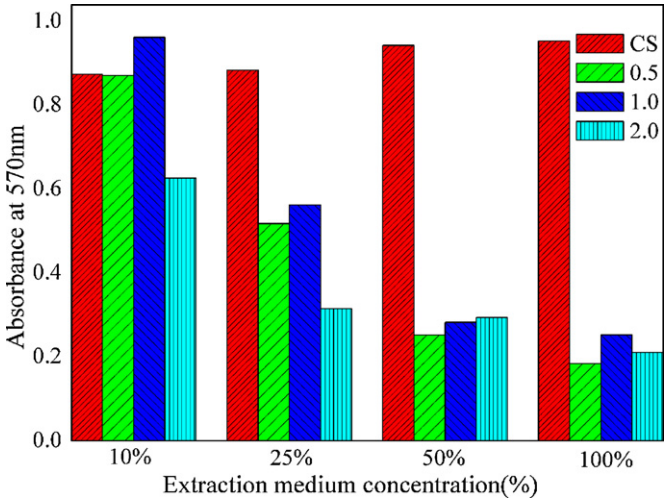

Fig. 7. Cytotoxicity test of PTX-loaded CS/HA electrospun nanofibers indirect cytotoxicity.

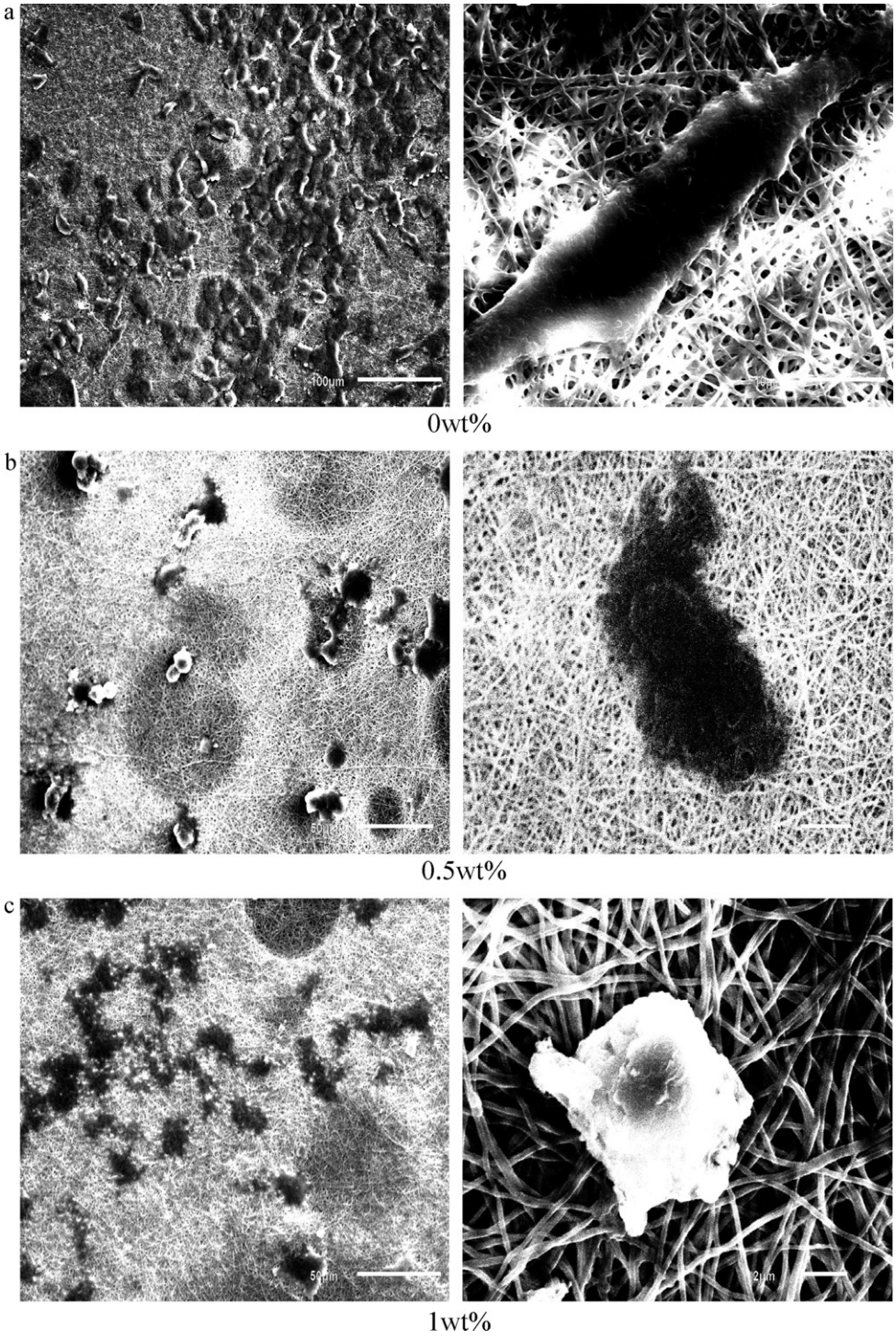

Fig. 8. SEM micrographs of DU145 prostate cancer cells attached to CS/HA nanofibers with different loaded PTX concentration after 48 .

3.7. Cell adhesion and proliferation

Cell morphology of the DU145 prostate cancer cells treated by PTX-loaded/CS–HA nanofibers mats after 48 h cell culture was shown in Fig. 8. The blank CS–HA nanofibers mat did not show any cytotoxicity to DU145 prostate cancer cells compared with the control. It could be found that, DU145 prostate cancer cells appeared to adhere well and exhibited a normal morphology on the nanofibers, which was due to the lots of porous, rough surfaces of the fibers assist in adhesion and proliferation of more number of cells (Gupta et al., 2009; Yang et al., 2004). DU145 prostate cancer cells attached on the surfaces by discrete filopodia, exhibited short and numerous microvilli on their surfaces, and tended to attach and grow along the polymer nanofibers. Those of the DU145 prostate cancer cells on nanofibers encapsulated by PTX were also included for comparison. In the case of 0.05%, 0.1% PTX-loaded/CS–HA nanofibers mats, the released amount of PTX was enough to inhibit the cells growth, so the cell numbers decreased rapidly during the test and the cells became more irregular shape. Cells spreading became more prominent and cells became in a flat morphology on the scaffold surface. Nanofibers mats loaded with more PTX showed stronger cell growth inhibition. These results strongly suggested that the

nanofibrous scaffolds reported here was suitable for postoperative chemotherapy of prostate cancer cancers.

4. Conclusions

In the paper, the characterization of electrospun CS/HA nanofibers was investigated in detail. The result from SEM images showed that porous morphology of the electrospinning nanofibers could be obtained by remove PEO via a selective dissolution technique with water. The structure and interaction between positive and negative charges of the fibers were subjected to detailed analysis by DSC and FT-IR. The result showed that interaction formed between the positively charged porous polymer (CS) nanofibers and negatively charged polymers (HA). Fluorescence for electrospun nanofibers results demonstrated PTX was dispersed inner of the nanofibers. The drug burst release behaviour was mainly related with adsorption of the nanofibers. DU145 prostate cancer cells attached on the surfaces, but cell numbers decreased with increase of concentration of encapsulation PTX owing to the inhibition growth.

Acknowledgements

The author would like to thank the project supported by the Natural Science Foundation of Jiangsu Province (BK2010190) for its financial support. This study was supported by Open Fund from State Key Laboratory of Chemical Resource Engineering, Beijing University of Chemical Technology.

References

Allison, D. D., & Grande-Allen, K. J. (2006). Hyaluronan: A powerful tissue engineering tool. *Tissue Engineering*, *12*, 2131–2140 (review).

Bhattarai, N., Edmondson, D., Veiseh, O., Matsen, F. A., & Zhang, M. Q. (2005). Electrospun chitosan-based nanofibers and their cellular compatibility. *Biomaterials*, *26*, 6176–6184.

Blasinska, A., & Drobnik, J. (2008). Effects of nonwoven mats of di-o-butyrylchitin and related polymers on the process of wound healing. *Biomacromolecules*, *9*, 776–782.

Bognitzki, M., Frese, T., Steinhart, M., Greiner, A., & Wendorff, J. H. (2001). Preparation of fibers with nanoscaled morphologies: Electrospinning of polymer blends. *Polymer Engineering &Science*, *41*, 982–989.

Chen, W. Y. J., & Abatangelo, G. (1999). Functions of hyaluronan in wound repair. *Wound Repair Regeneration*, *7*, 79–89.

Chen, Z. G., Wang, P. W., Wei, B., Mo, X. M., & Cui, F. Z. (2010). Electrospun collagen–chitosan nanofiber: A biomimetic extracellular matrix for endothelial cell and smooth muscle cell. *Acta Biomaterialia*, *6*, 372–382.

Fernando, R. D. A., & Sérgio, P. C. (2004). Characteristics and properties of carboxymethylchitosan. *Carbohydrate Polymers*, *75*, 214–221.

Gupta, D., Venugopal, J., Prabhakaran, M. P., Giri, Dev, V. R., Low, S., et al. (2009). Aligned and random nanofibrous substrate for the in vitro culture of Schwann cells for neural tissue engineering. *Acta Biomaterialia*, *5*, 2560–2569.

Hong, J. K., & Madihally, S. V. (2010). Three-dimensional scaffold of electrosprayed fibers with large pore size for tissue regeneration. *Acta Biomaterialia*, *6*, 4734–4742.

Huang, Z. M., Zhang, Y. Z., Ramakrishna, S., & Lim, C. T. (2004). Electrospinning and mechanical characterization of gelatin nanofibers. *Polymer*, *45*, 5361–5368.

Im, J. S., Yun, J., Lim, Y. M., Kim, H. I., & Lee, Y. S. (2010). Fluorination of electrospun hydrogel fibers for a controlled release drug delivery system. *Acta Biomaterialia*, *6*, 102–109.

Khor, E., & Lim, L. Y. (2003). Implantable applications of chitin and chitosan. *Biomaterials*, *24*, 2339–2349.

Kurpinski, K. T., Stephenson, J. T., Janairo, R. R., Lee, H., & Li, S. (2010). The effect of fiber alignment and heparin coating on cell infiltration into nanofibrous PLLA scaffolds. *Biomaterials*, *31*, 3536–3542.

Li, D., Wang, Y. L., & Xia, Y. N. (2004). Electrospinning nanofibers as uniaxially aligned arrays and layer-by-layer stacked films. *Advanced Materials*, *16*, 361–366.

Manna, U., Bharani, S., & Patil, S. (2009). Layer-by-layer self-assembly of modified hyaluronic acid/chitosan based on hydrogen bonding. *Biomacromolecules*, *10*, 2632–2639.

Meng, Z. X., Xu, X. X., Zheng, W., Zhou, H. M., Li, L., Zheng, Y. F., et al. (2011) Preparation and characterization of electrospun PLGA/gelatin nanofibers as a potential drug delivery system. *Colloids and Surfaces B: Biointerfaces* (on line), 84, 97-102.

Meyer, K. (1947). The biological significance of hyaluronic acid and hyaluronidase. *Physiological Reviews*, *27*, 335–359.

Mu, L., Teo, M. M., Ning, H. Z., Tan, C. S., & Feng, S. S. (2005). Novel powder formulations for controlled delivery of poorly soluble anticancer drug: Application and investigation of TPGS and PEG in spray-dried particulate system. *Journal of Controlled Release*, *103*, 565–575.

Pan, C., Ge, L. Q., & Gu, Z. Z. (2007). Fabrication of multi-walled carbon nanotube reinforced polyelectrolyte hollow nanofibers by electrospinning. *Composites Science and Technology*, *67*, 3271–3277.

Ranganath, S. H., & Wang, C. H. (2008). Biodegradable microfiber implants delivering paclitaxel for post-surgical chemotherapy against malignant glioma. *Biomaterials*, *29*, 2996–3003.

Reneker, D. H., & Chun, I. (1996). Nanometre diameter fibres of polymer, produced by electrospinning. *Nanotechnology*, *7*, 216–223.

Senel, S., & McClure, S. J. (2004). Potential applications of chitosan in veterinary medicine. *Advanced Drug Delivery Reviews*, *56*, 1467–1480.

Shalumon, K. T., Binulal, N. S., Selvamurugan, N., Nair, S. V., Menon, D., Furuike, T., et al. (2009). Electrospinning of carboxymethyl chitin/poly(vinyl alcohol) nanofibrous scaffolds for tissue engineering applications. *Carbohydrate Polymers*, *77*, 863–869.

Sill, T. J., & Recum, H. A. (2008). Electrospinning: Applications in drug delivery and issue engineering. *Biomaterials*, *29*, 1989–2006.

Sujata, S., Chung, C., Khetan, S., & Burdick, J. A. (2008). Hydrolytically degradable hyaluronic acid hydrogels with controlled temporal structures. *Biomacromolecules*, *9*, 1088–1092.

Theron, J. P., Knoetze, J. H., Sanderson, R. D., Hunter, R., Mequanint, K., Franz, T., et al. (2010). Modification, crosslinking and reactive electrospinning of a thermoplastic medical polyurethane for vascular graft applications. *Acta Biomaterialia*, *6*, 2434–2447.

Tiwaria, S. K., Tzezanab, R., Zussmanb, E., & Venkatramana, S. S. (2010). Optimizing partition-controlled drug release from electrospun core–shell fibers. *International Journal of Pharmaceutics*, *392*, 209–217.

Toole, B. P. (2004). Hyaluronan: From extracellular glue to pericellular cue. *Nature Reviews Cancer*, *4*, 528–539.

Velde, K. V., & Kiekens, P. (2004). Structure analysis and degree of substitution of chitin, chitosan and dibutyrylchitin by FT-IR spectroscopy and solid state 13C NMR. *Carbohydrate Polymers*, *58*, 409–416.

Wongsasulak, S., Kit, K. M., McClements, D. J., Yoovidhya, T., & Weiss, J. (2007). The effect of solution properties on the morphology of ultrafine electrospun egg albumene–PEO composite fibers. *Polymer*, *48*, 448–457.

Woon, W., Fong, L., Hung, C. H., & Yuen, P. T. (2010). Effect of face velocity, nanofiber packing density and thickness on filtration performance of filters with nanofibers coated on a substrate. *Separation and Purification Technology*, *71*, 30–37.

Worrall, E. E., Sudarisman, & Priadi, A. (2009). Sialivac: An intranasal homologous inactivated split virus vaccine containing bacterial sialidase for the control of avian influenza in poultry. *Vaccine*, *27*, 4161–4168.

Yang, F., Murugan, R., Ramakrishna, S., Wang, X., Ma, Y. X., & Wang, S. (2004). Fabrication of nano-structured porous PLLA scaffold intended for nerve tissue engineering. *Biomaterials*, *25*, 1891–1900.

Yang, F., Murugan, R., Wang, S., & Ramakrishna, S. (2005). Electrospinning of nano/micro scale poly(L-lactic acid) aligned fibers and their potential in neural tissue engineering. *Biomaterials*, *26*, 2603–2610.

Yoo, H. S., Lee, E. A., Yoon, J. J., & Park, T. G. (2005). Hyaluronic acid modified biodegradable scaffolds for cartilage tissue engineering. *Biomaterials*, *26*, 1925–1933.

You, Y., Youk, J. H., Lee, S. W., Min, B. M., Lee, S. J., & Park, W. H. (2006). Preparation of porous ultrafine PGA fibers via selective dissolution of electrospun PGA/PLA blend fibers. *Materials Letters*, *60*, 757–760.

Yui, T., Kobayashi, H., Kitamura, S., & Imada, K. (1994). Conformational analysis of chitobiose and chitosan. *Biopolymers*, *34*, 203–208.

Zhang, Y. Z., Venugopal, J., Huang, Z. M., Lim, C. T., & Ramakrishna, S. (2006). Crosslinking of the electrospun gelatin nanofibers. *Polymer*, *47*, 2911–2917.

Zhou, Y. S., Yang, D. Z., Chen, X. M., Xu, Q., Lu, F. M., & Nie, J. (2008). Electrospun water-soluble carboxyethyl chitosan/poly(vinyl alcohol) nanofibrous membrane as potential wound dressing for skin regeneration. *Biomacromolecules*, *9*, 349–354.